Strategies to unblock the n-GaAs surface when electrodepositing Bi from acidic solutions

Alicia Prados , Rocío Ranchal , Lucas Pérez

ABSTRACT

Bismuth ultra-thin films grown on n-GaAs electrodes via electrodeposition are porous due to a blockade of the electrode surface caused by adsorbed hydrogen when using acidic electrolytes. In this study, we discuss the existence of two sources of hydrogen adsorption and we propose different routes to unblock the n-GaAs surface in order to improve Bi films compactness. Firstly, we demonstrate that increasing the electrolyte temperature provides compact yet polycrystalline Bi films. Cyclic voltammetry scans indicate that this low crystal quality might be a result of the incorporation of Bi hydroxides within the Bi film as a result of the temperature increase. Secondly, we have illuminated the semiconductor surface to take advantage of photogenerated holes. These photocarriers oxidize the adsorbed hydrogen unblocking the surface, but also create pits at the substrate surface that degrade the Bi/GaAs interface and prevent an epitaxial growth. Finally, we show that performing a cyclic voltammetry scan before electrodeposition enables the growth of compact Bi ultra-thin films of high crystallinity on semiconductor substrates with a doping level low enough to perform transport measurements.

1. Introduction

Bismuth nanostructures have received much attention in recent years due to the fascinating changes in electronic properties observed at the nanoscale [1] [2] [3] [4]. Bi ultra-thin films are expected to behave as topological insulators [5] and, in fact, topological edge states have already been observed in Bi bilayers [6] [7]. These topologically protected surface states, strongly spin-polarized via Rashba interaction [8] [9], make Bi a very interesting material for the future design of spintronics devices [10]. Very recently, a large spin to charge conversion induced by spin-orbit coupling in a Bi/Ag Rashba interface [11] has been measured.

Among the different methods for the synthesis of Bi, electrodeposition has appeared as a very effective one as it provides high-quality Bi nanostructures which have allowed the measurement of quantum transport in electrodeposited Bi nanowires [12] [13]. However, the study of the previously mentioned 2D effects requires the growth of continuous high quality Bi films with a thickness lower than the wavelength of the electrons at the Fermi level (λ_F(Bi) = 40-70 nm). In addition, these ultra-thin Bi films must be electrically isolated from the substrate in order to prevent current leakage during the measurements. The latter is guaranteed through the use of middle and low-doped semiconducting substrates ($N_D < 1{\cdot}10^{18}\,cm^{-3}$), which provides wide Bi/semiconductor Schottky barriers. Although Bi/n-GaAs diodes have already been obtained via electrodeposition [14] [15] [16], there are no quantum transport studies of Bi ultra-thin films in this configuration. This lack of measurements could be related to a bad electrical isolation due to the high porosity of Bi ultra-thin films grown on n-GaAs electrodes. Lately, we have proved this porosity to be a consequence of the surface blockade of n-GaAs electrodes, probably caused by adsorbed hydrogen (H_{ads}) [17]. This adsorbed layer, formed as a result of the interaction between the n-GaAs surface and the acidic electrolyte, presents a high stability due to the covalent nature of the As-H bond. Consequently, this layer blocks the substrate surface until the overpotential is high enough to promote hydrogen desorption by a second discharge of protons (Volmer-Heyrovsky route [18]), hindering the deposition of species with a more positive reduction potential (i.e. Bi, Ag, Au), which leads to porous and poor quality ultra-thin films [17] [19] [20]. In the case of Bi, the presence of the H_{ads} layer cannot be avoided by increasing the electrolyte pH because acidic electrolytes must be used. On one hand, Bi oxide and Bi salts are only soluble in strong acids and on the other hand, Bi solutions become unstable if they are treated with alkaline solutions because $Bi_2O_3{\cdot}x(H_2O)$ precipitates as white flakes [21]. Therefore, it is necessary to remove the

H_{ads} layer before the film is deposited in order to obtain compact films. This constitutes the first step for the growth of high-quality Bi ultra-thin films.

In this work we present three routes to promote the H_{ads} layer desorption with the purpose of obtaining compact 50 nm Bi films using acidic electrolytes: first with an increase of the electrolyte temperature (temperature route), second by illuminating the substrate before the film growth (light route), and third by carrying out a voltage scan before growing the film (voltage scan route). Our experimental results show that the best protocol is the voltage scan route as it does not alter the substrate surface and provides films with higher structural quality than the other two routes. In addition, we discuss the existence of two sources of hydrogen adsorption: the transferred charge necessary to reach the electrochemical equilibrium and the interaction between As-derived surface states and electrolyte protons (responsible for hydrogen readsorption).

2. Experimental methods

Electrochemical experiments have been carried out using a stable water-based electrolyte containing 1 mM Bi_2O_3 (bismuth oxide) as BiO^+ source and 1 M $HClO_4$ (perchloric acid) as supporting electrolyte. It is especially convenient to use perchloric acid because ClO_4^- ions do not tend to form complexes with Bi ions (unlike HCl, H_2SO_4 or HNO_3) [21] besides they do not tend to get specifically adsorbed on electrodes surfaces [22] [23]. Solutions were prepared with analytical grade chemicals and deionized water in order to avoid free ions. Bismuth oxide was firstly added to perchloric acid in a volumetric flask and then, the solution was made to the mark with deionized water. The pH of the solution (approximately 0.1) was not necessary to be further adjusted. The BiO^+ solution is not deaerated since oxygen does not seem to play a role on the GaAs surface blockade. In addition, dissolved oxygen cannot produce Bi oxide since this is highly soluble in strong acid solutions as the one used in this study. Finally, other authors have used non-deaerated solutions (both at room temperature and at 343 K) for the electrodeposition of Bi on n-GaAs substrates and no evidences of an interfacial oxide layer nor oxygen in the films have been detected [15] [24].

Working electrodes were Si doped n-type GaAs (111)B wafers, supplied by Geo Semiconductors, with a donor density of $N_D \sim (0.6 - 1)\cdot 10^{18}\,cm^{-3}$. Ohmic contacts were made on the back of the wafers by thermal evaporation of 80 nm of AuGe and 250 nm of Au, followed by an annealing at 653 K (380 °C) in a mixture of 95% N_2 and 5% H_2 for 90 s. Prior to each experiment, substrates were pre-treated as described in reference [17] in order to achieve a flat oxide-free As-rich surface. The substrate surface was protected from air with a drop of 1 M $HClO_4$ (supporting electrolyte) when transferred to the BiO^+ solution, where substrates stayed approximately 1 minute in darkness to reach a stable OCP. Unless otherwise stated, all experiments were performed without agitation, at 300 K and in darkness. When illumination was needed for the experiment, white light (white LED, 220 lm, T_c = 2700-3500 K) was switched on just a few seconds before starting the experiment.

Electrochemical experiments were performed in a three-electrode cell with a platinum mesh as counter electrode and a Ag/AgCl (3 M NaCl) reference electrode supplied by BASi (E_{eq} = 0.196 V vs. SHE). In this study, all potentials are referred to this electrode. Electrochemical experiments were controlled by a Metrohm Autolab PGSTAT302N potentiostat. The nominal thickness of the films was controlled by Faraday's law considering a deposition efficiency of 100%. After deposition, films were dipped in $HClO_4$, rinsed in deionized water and dried with N_2.

Surface characterization was done by both Nanotec and Nanoscope Atomic Force Microscopes (AFM) with a Si tip, in tapping mode and operating in air. Images were analyzed with WSxM 5.0 software and Nanoscope 5.31r1 software.

Structural characterization was done by X-ray Diffraction using a Philips X'Pert PRO system equipped with a Cu target ($\lambda_{K\alpha}$ = 1.54 nm) and a four-circle goniometer. All films have been measured in

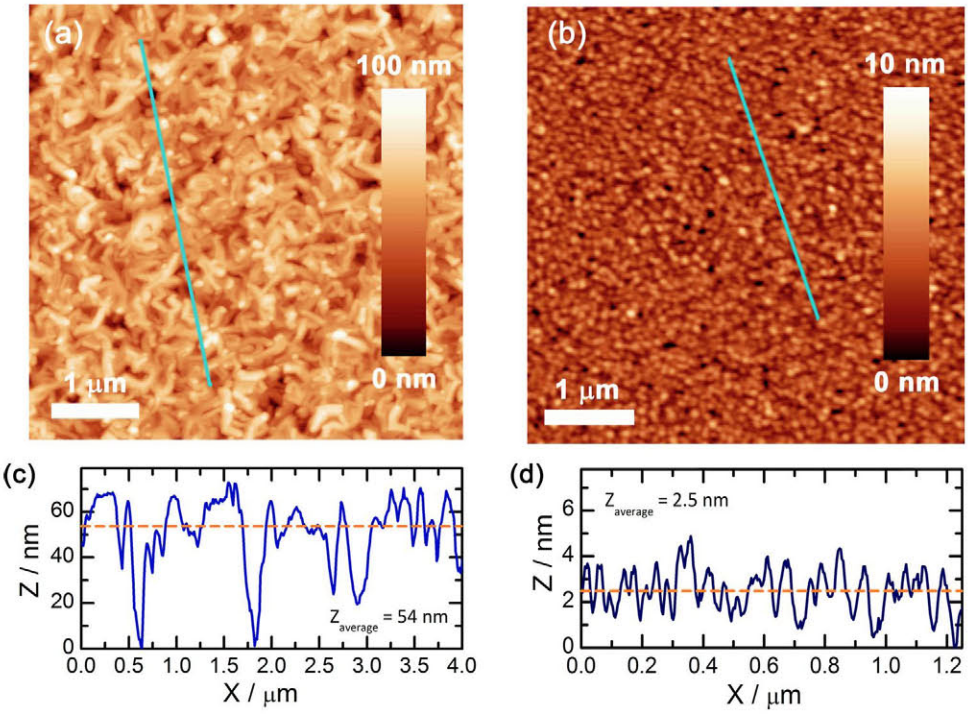

Fig. 1. AFM images of a) 50 nm Bi film grown at −0.2 V in darkness and at 300 K, b) n-GaAs surface after carrying out substrates pretreatment. (c) and (d) are the AFM depth profiles measured in the marked lines in (a) and (b), respectively.

grazing incidence mode (GIXRD), also called grazing incidence asymmetric-Bragg diffraction (GIABD). The grazing angle of X-ray incidence was set in the range of 0.3–1° and the detector scanned in the 2θ range from 20° to 90°. In addition, those films with only a few reflections in their GIXRD pattern were also measured in Bragg-Brentano configuration (ω-2θ scan) to corroborate the presence of preferred orientations. To avoid substrate reflections, an offset of 0.5° was introduced between the incidence and the diffracted direction ($\omega = \theta - \theta_{offset}$).

3. Results and discussion

As we have previously discussed, porous Bi films are obtained when electrodepositing on n-GaAs substrates in darkness at 300 K. Fig. 1.a shows an AFM image of a 50 nm Bi film grown at −0.2 V under these conditions. This film presents a high roughness for a film of this thickness (rms = 12 nm) despite the n-GaAs surface after the pretreatment is homogeneous and flat (rms = 2 nm) (Fig. 1. b and d). AFM depth profiles of the Bi sample also show areas with a depth higher than the nominal film thickness (Fig. 1.c), indicating an incomplete substrate coverage. The Bi layers obtained in this case are polycrystalline (Fig. 2.a) as a result of the hindered nucleation caused by the presence of the H_{ads} layer.

3.1. Temperature route

A common method to improve the crystal quality of a film is to increase the thermal energy of the system during the growth stage. This enhances adatoms diffusion along the substrate surface and allows them to find suitable positions. Therefore, we propose to increase the electrolyte temperature as the first strategy to improve Bi thin films compactness and crystal quality. In order to confirm the validity of this route, a 50 nm Bi film was grown at −0.2 V and 323 K. AFM images (Fig. 3.a and b) show a compact film whose islands present diffuse boundaries, as a result of a higher coalescence produced by the temperature increase. Film roughness (rms) has decreased to 6 nm and AFM depth profiles show the substrate is well covered (Fig. 3.c and d). Nevertheless, XRD measurements evidence that this layer is polycrystalline and two broad peaks can be observed at 2θ = 53° and 2θ = 85.6° (Fig. 2.c).

Fig. 4.a shows two cyclic voltammetries (CV) performed at 300 K and at 323 K at a scan rate of 10 mV/s. Both CVs start at the OCP (90 mV and 120 mV, respectively), go first till $E_1 = -0.8$ V, then to $E_2 = 0.8$ V and finish at the OCP. At 300 K there is a shift between consecutive scans of approximately 75 mV that is related to the blockade of the substrate surface by the H_{ads} layer [17]. The CV carried out at 323 K also shows a shift between scans (~30 mV), though it is smaller than the shift obtained at 300 K. This confirms that the H_{ads} atoms diffusion is not enhanced by the temperature increase, as expected from the As-H covalent bond. Consequently, the n-GaAs surface is still blocked when the Bi layer starts to grow (i.e. the nucleation is hindered), which results in a polycrystalline layer as observed in the XRD data. Nonetheless, the onset potential at 323 K (-100 mV) is lower that at 300 K (-220 mV) which means that the limiting step of the Volmer-Heyrovsky route ($H_{ads} + H^+ + e^- \rightarrow H_2$) is enhanced by the temperature increase. Then, BiO^+ ions can get reduced faster than at 300 K (at the same growth potential), leading to a higher coalescence (Fig. 3.a and b).

The CV performed at 323 K also presents four extra reduction peaks at potentials $E_{(1)} \approx -0.13$ V, $E_{(2)} \approx -0.29$ V, $E_{(3)} \approx -0.43$ V and $E_{(4)} \approx -0.55$ V (Fig. 4.a). These peaks are not present in a CV performed in the supporting electrolyte at the same temperature (Fig. 4.b), which means that they are not related to convection effects or to ClO_4^- ions. Besides, these extra peaks are present in a CV carried out in a deaerated BiO^+ solution (not shown), which indicates that they are not linked to dissolved oxygen. Moreover, these peaks appear when using a Au substrate (Fig. 4.b), which implies that they are not a consequence of a chemical change of the GaAs surface (i.e. GaAs oxidation). Taking into account these results, we attribute these extra peaks to the reduction of different Bi hydroxy complexes into metallic Bi [25]. These complexes, probably unstable at room temperature at this pH [26], might be formed as a result of the temperature increase. The broad peaks observed in the XRD patterns suggest that some of these complexes are incorporated within the Bi film during its growth, being responsible for its polycrystallinity.

In conclusion, although this route leads to continuous films, the occurrence of new electrochemical reactions might lead to the incorporation of Bi hydroxides within the Bi film, which decreases the crystal quality of the layer. Therefore, this route does not seem appropriate for the electrodeposition of high quality Bi films.

3.2. Light route

We have already shown that the n-GaAs surface is unblocked by photogenerated holes [27] when it is illuminated while being

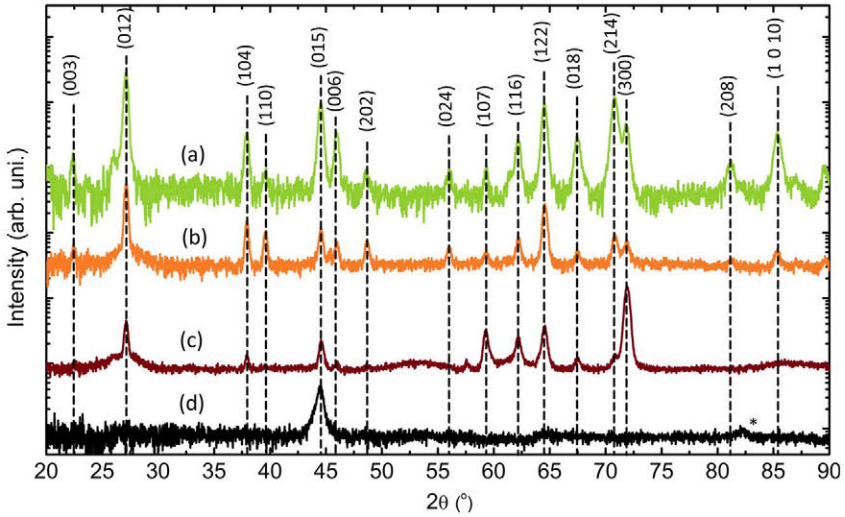

Fig. 2. GIXRD patterns of 50 nm Bi films grown on n-GaAs(111)B under different conditions: a) in darkness, at 300 K and at −0.2 V; b) under illumination, at 300 K and −0.3 V; c) in darkness, at 323 K and at −0.2 V; d) after performing a CV scan, in darkness, at 300 K and at −0.2 V. The dashed lines indicate the position of Bi reflections (ICDD card 00-044-1246) that matches with an observed peak. The peak marked with an * in the pattern (d) corresponds with the As(009) reflection.

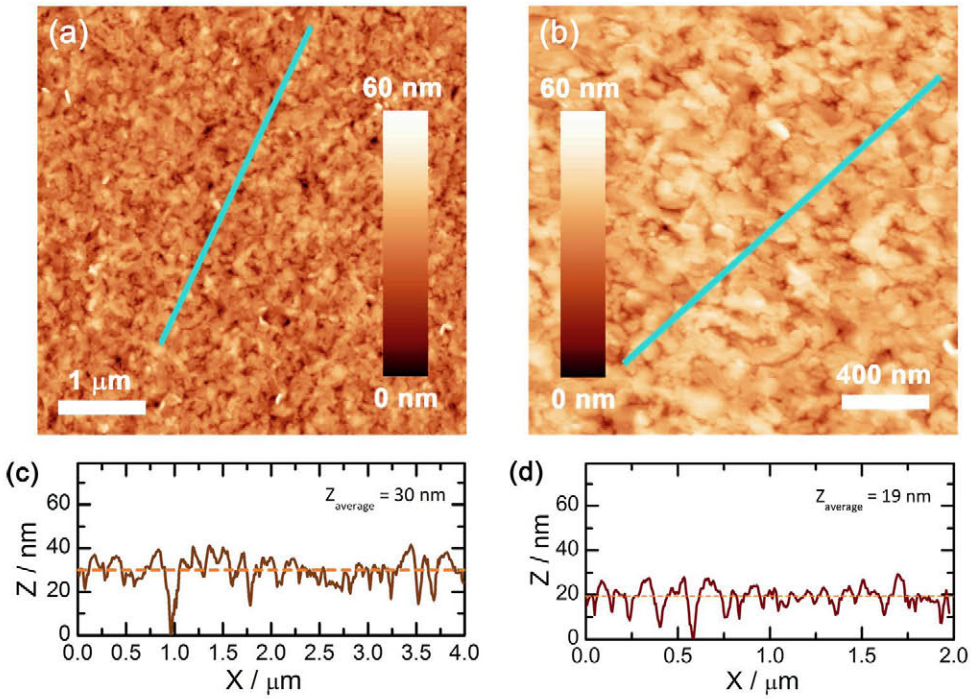

Fig. 3. AFM images and depth profiles of a 50 nm Bi thin film grown on n-GaAs(111)B at −0.2 V at 323 K. a) Scan size of 5 × 5 μm². b) Scan size of 2 × 2 μm². (c) and (d) are the depth profiles obtained from the lines marked in (a) and (b), respectively.

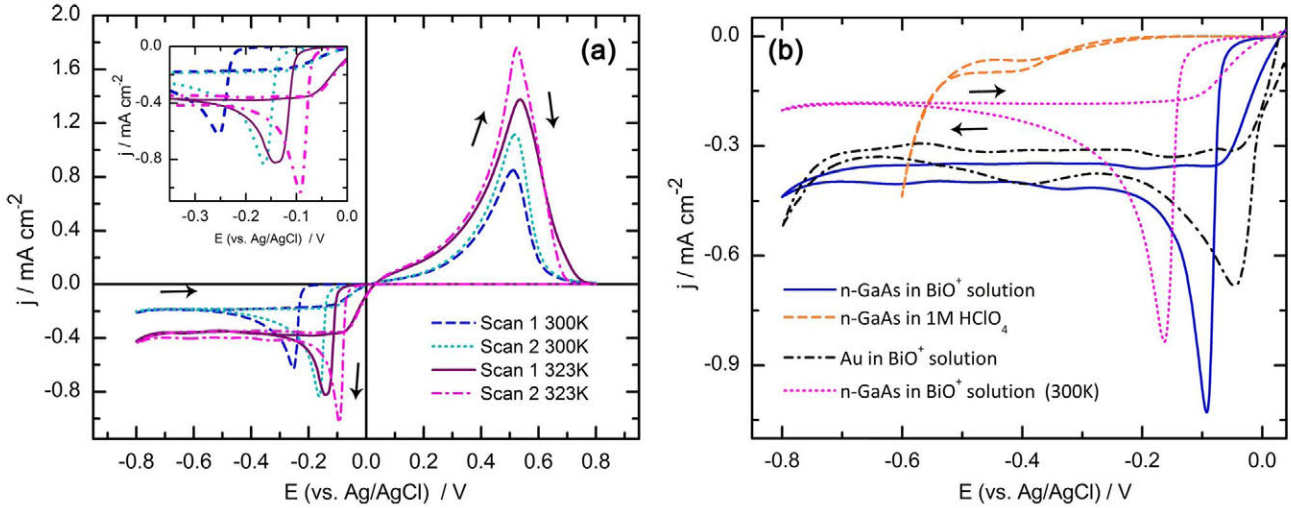

Fig. 4. a) CV scans for n-GaAs(111)B in BiO^+ solution performed at two different temperatures and at a scan rate of 10 mV/s. The inset is an enlargement to clearly show the reduction peaks. b) Cathodic stage of CV scans for n-GaAs(111)B and Au substrates in the BiO^+ solution and in the supporting electrolyte (1 M $HClO_4$) at 323 K in darkness. Scan rate of 10 mV/s in all cases.

immersed in the electrolyte [17]. Hence, it seems that compact Bi films can be obtained if the n-GaAs surface is illuminated before (and maybe during) the film growth since it will lead to a hydrogen-free surface before the growth starts. To check this route, a 50 nm Bi film was grown under illumination conditions. Illumination was switched on a few seconds before the growth started and it was maintained during the whole growth. In this case, the applied potential was −0.3 V because the OCP under this illumination was −0.29 V. This Bi film presents well-arranged triangle-shaped islands (Fig. 5.a), consistent with the trigonal Bi crystal symmetry, with larger sizes (150 - 350 nm) than those obtained in reference [15]. We associate these large and well-arranged islands to the slow deposition rate achieved in this growth as a result of two effects: Bi-Bi bonds break because of photogenerated holes and the small overpotential applied (10 mV). As a result, Bi atoms have more time to find a suitable position, which leads to a better atomic arrangement to reach the natural trigonal symmetry of bulk bismuth. The film exhibits a high roughness (rms ≈ 12 nm) for a 50 nm thick layer, but it shows a higher compactness and a higher substrate coverage than the film obtained in dark conditions (Fig. 1.a) as indicated by AFM depth profiles (Fig. 5.a and c).

Although the morphology of the film has been improved, XRD measurements show that this film is polycrystalline (Fig. 2.c). We deduce that this characteristic is a result of the surface damage caused by illumination. AFM images show the appearance of pits at the n-GaAs surface after illuminating it during 170 s while it was immersed in the BiO^+ solution at OCP conditions (Fig. 5.b and d).

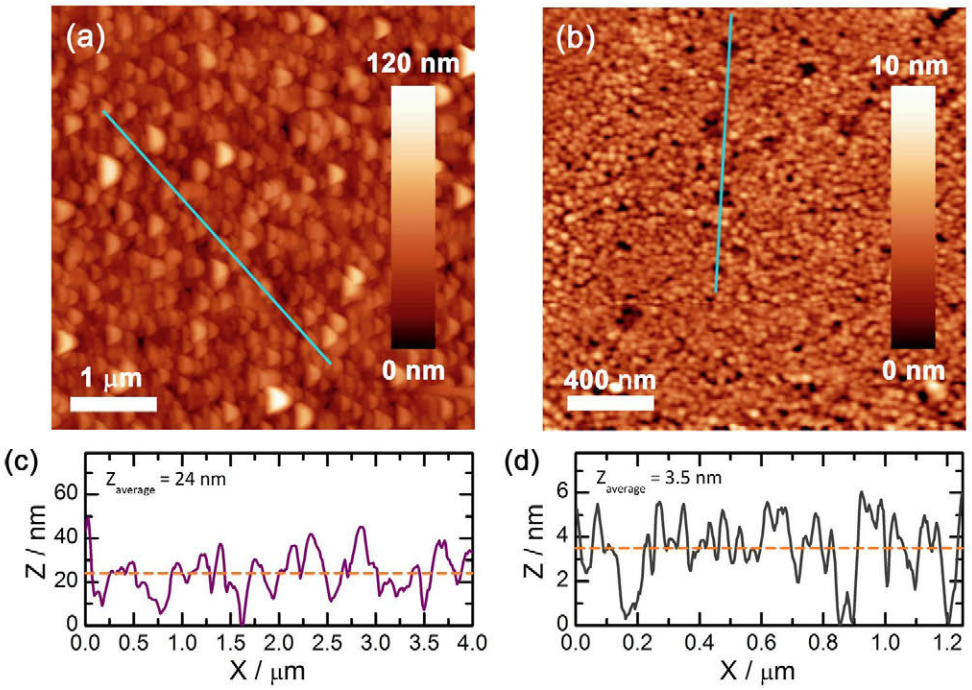

Fig. 5. AFM images and depth profiles of a (a) 50 nm Bi film grown on n-GaAs(111)B under illumination conditions at −0.3 V, (b) n-GaAs(111)B surface after illuminating it for 170 s while it was immersed into the BiO^+ solution. (c) and (d) are the depth profiles obtained from the lines marked in (a) and (b), respectively.

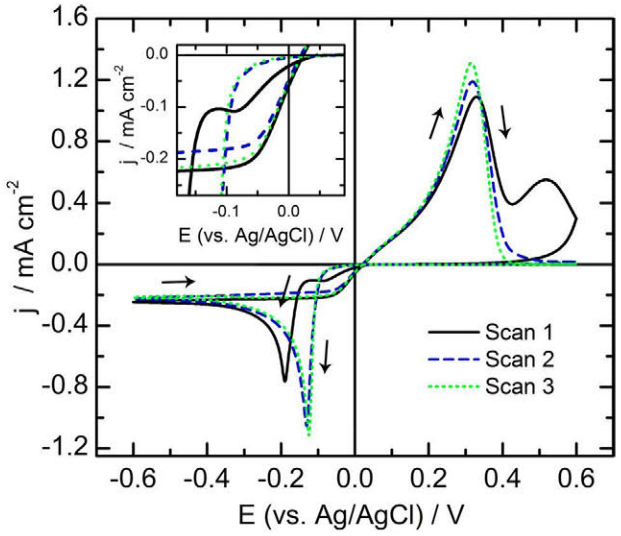

Fig. 6. CV scans for n-GaAs(111)B in BiO^+ solution performed at 10 mV/s under dark conditions but after illuminating the substrate for 400 s (white LED, 220 lm, T_c = 2700-3500 K). The CV starts at the OCP ≈ 45 mV and sweeps first till E_1 = −0.6 V; then the scan is reversed and goes up to E_2 = 0.6 V and returns to the OCP to start the next scan. The inset is an enlargement to clearly show the new cathodic peak that appears in the first scan.

Fig. 6 also shows the appearance of two additional peaks just in the first scan of a CV performed in darkness but after illuminating the substrate for 400 s: one cathodic (E_{onset} ~ 15 mV) and one anodic (E_{onset} ~ 200 mV, value that has been estimated by carrying out a Lorentzian deconvolution of the two anodic peaks). These peaks have already been observed by other authors, being attributed to the formation of a passivating layer at the n-GaAs surface as a result of prolonged illumination [28] [29]. As mentioned above, when an n-GaAs electrode is illuminated, photogenerated holes go towards the substrate surface and break As-H bonds. When all As-H bonds have been broken, photogenerated holes start to break As-Ga bonds, leading to lattice decomposition [30] [31] and giving rise to n-GaAs (photo) corrosion [32] [33]. We have measured the OCP as a function of time when the substrate goes from darkness to illumination and we estimate that the complete removal of the H_{ads} by photogenerated holes takes approximately 20 s, which is in agreement with a previous work [34] (taking into account the difference in substrate doping level and, probably, in light intensity). The situations shown in Fig. 5.b (formation of pits) and Fig. 6 (formation of a passivating layer) occur after illuminating the substrate for 170 s and 400 s, respectively, being therefore a consequence of the substrate photocorrosion. Erné et al. [35] suggest that the reactions involved in n-GaAs photocorrosion (in acidic solutions) are:

$$GaAs + 2H_2O + 6h^+ \rightarrow Ga^{3+}_{aq} + HAsO_{2(aq)} + 3H^+ \qquad \text{(reaction 1)}$$

$$GaAs + 3h^+ \rightarrow Ga^{3+}_{(aq)} + As^0_{(s)} \qquad \text{(reaction 2)}$$

Ga^{3+}, $HAsO_{2(aq)}$ and H^+ are soluble products that diffuse into the bulk solution. However, since As^0 is insoluble either in water or in acidic solutions, it will remain on the substrate surface forming an amorphous layer [35] [36]. Since similar features have been observed for n-GaAs substrates in H_2SO_4:H_2O_2 solutions under illumination [28], we can assume that in our case the As^0 layer becomes partial or completely oxidized by dissolved oxygen and, therefore, the extra cathodic peak observed in Fig. 4 might be assigned to reaction 3 (reduction potential around 30 mV [37]):

$$As_2O_3 + 6H^+ + 6e^- \rightarrow 2As + 3H_2O \qquad \text{(reaction 3)}$$

On the other hand, the extra anodic peak could be assigned to the dissolution of the As^0 via reaction 4 (oxidation potential around 50 mV [37]):

$As + 2H_2O + 3h^+ \rightarrow HAsO_{2(aq)} + 3H^+$ (reaction 4)

It should be pointed out that our films grown under illumination conditions do not show amorphous phases (due to the As^0 layer) nor traces of As oxide in XRD measurements (Fig. 2.b). Since illumination is switched on a few seconds before the growth starts, little photocorrosion might take place during the first stages of the growth and the small amount of resulting products would not be detectable by XRD. Besides, reaction 3 occurs rather quickly at the potential applied in this growth (−0.3 V), so no traces of As oxide will remain.

It can be concluded that illuminating the substrate provides compact Bi ultra-thin films with well-arranged islands but with a bad Bi/n-GaAs interface. GaAs photocorrosion leads to the formation of an amorphous As layer that prevents an epitaxial growth. Besides, the emergence of pits on the substrate surface increases its roughness (Fig. 5.b), deteriorating the Bi layer morphology. These pits could also create interfacial states between the Bi and the n-GaAs, inducing energy levels in the band gap and causing the pinning of the Fermi level. Thus, electrons could cross over the Schottky barrier through these interfacial states, which can be seen as a lowering of the Schottky barrier height. Therefore, the use of illumination to grow Bi films should be ruled out as a consequence of the rough Bi films that are obtained and the non-appropriate electrical isolation between the film and the substrate.

3.3. Voltage scan route

In the light of the previous results, it is necessary to find a new route which does not damage the substrate surface when desorbing the H_{ads} layer in order to provide good enough film/substrate interfaces. In a previous study we showed that the n-GaAs surface blockade caused by an adsorbed hydrogen layer is reflected in a CV as a shift between the first and the subsequent scans [17]. The absence of shifts between the successive CV scans confirms that the H_{ads} layer is removed after performing the first one. Taking into account this result, we propose to carry out a CV scan just before growing the Bi ultra-thin film as a strategy to improve its compactness. In this procedure, the CV scan starts at the OCP (≈ 100 mV) and sweeps in first place to $E_1 = -0.6$ V. Then the potential is reversed and goes up to $E_2 = 0.6$ V to dissolve all the Bi electrodeposited during the cathodic stage. Finally, the CV ends at the OCP and immediately the Bi layer is grown at −0.2 V (without opening the cell). On the contrary to the previously proposed routes, this one does not damage the substrate surface (Fig. 7.a) nor does it lead to the formation of different Bi hydroxy complexes since it is carried out at 300 K and in darkness (Fig. 4). The morphology of the Bi layer grown following this procedure (Fig. 7.b) is completely different from the morphology of a Bi layer grown at the same conditions but without carrying out a previous CV (Fig. 1.b). Fig. 7.b shows rounded islands with a wide size distribution (d = 100-500 nm) whereas Fig. 1.b shows elongated islands with a narrower size distribution (L = 430-570 nm; d = 280-300 nm). Although rms and peak-to-valley values are quite similar in both films (rms ~12 nm and PV ~125 nm), depth profiles clearly show that in Fig. 7.b the substrate is completely covered whereas in Fig. 1.b it is not. Moreover, the film grown following the scan route presents an XRD pattern with only one significant reflection assigned to the Bi(015) direction and two small contributions assigned to the Bi(122) and the As(009) reflections (Fig. 2.d). This absence of Bragg peaks when using out-of-plane GIXRD usually indicates the existence of a preferred orientation parallel to the substrate surface [38]. Therefore, we have performed symmetric (Bragg-Brentano) measurements in this film and the pattern obtained verify a Bi(012) texture (Fig. 8). These results confirm that this route improves the compactness and also the crystal quality of the Bi ultra-thin film due to an enhancement of the nucleation mechanism as a result of the absence of the adsorbed hydrogen layer when starting the Bi growth.

When following this route it should be taken into account that n-GaAs anodic dissolution starts at approximately 1 V (it varies slightly depending on substrate doping level and on substrate

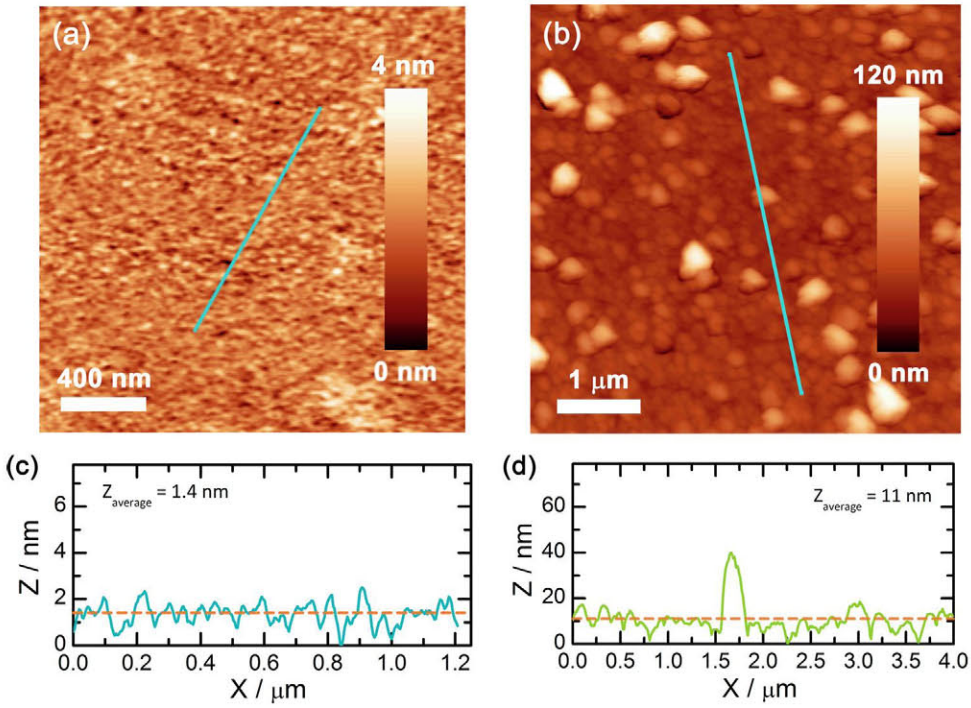

Fig. 7. AFM images and depth profiles of a a) n-GaAs (111)B surface after performing a CV scan in the BiO^+ solution b) 50 nm Bi film grown at −0.2 V on n-GaAs(111)B under dark conditions and at 300 K after performing a CV scan. (c) and (d) are the depth profiles obtained from the lines marked in (a) and (b), respectively.

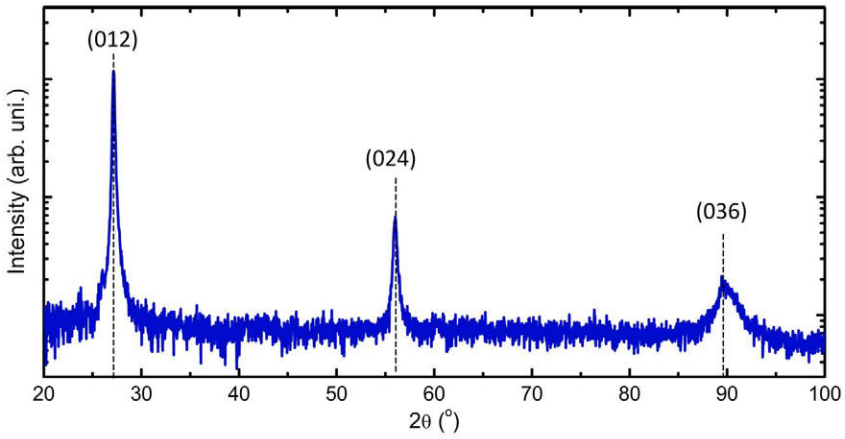

Fig. 8. XRD pattern of a 50 nm Bi film grown on n-GaAs(111)B after performing a CV scan, in darkness, at 300 K and at −0.2 V. The dashed lines indicate the position of Bi reflections (ICDD card 00-044-1246) that matches with the observed peaks.

orientation) which can lead to the formation of some oxides [39]. However, if the CV scan has a lower anodic reverse potential (E_2), the substrate remains oxide-free since no peaks assigned to reactions 3, 5 and 6 [37] are observed in the following scans [17]. In relation with n-GaAs anodization and as a consequence of the Schottky barrier formed at the n-GaAs/Bi interface, this routine is limited to high and middle-doped substrates ($N_D > 1 \cdot 10^{17}$ cm^{-3}). Since the Schottky barrier width increases inversely with the substrate doping level, substrates with low doping concentrations need higher anodic potentials to dissolve the electrodeposited Bi and GaAs anodization could take place. This would lead to a poor n-GaAs/Bi interface (poor Schottky barrier).

$$Ga_2O + 2H^+ + 2e^- \rightarrow 2Ga + H_2O \qquad (E_{Ag/AgCl} \approx -0.60V)$$

(reaction 5)

$$Ga_2O_3 + 6H^+ + 6e^- \rightarrow 2Ga + 3H_2O \qquad (E_{Ag/AgCl} \approx -0.7V)$$

(reaction 6)

Nevertheless, this routine allows the growth of high quality Bi films on semiconductor substrates with a doping level low enough to perform transport measurements ($N_D < 8 \cdot 10^{17}$ cm^{-3}).

3.4. Comparison of the three routes

All Bi films grown in this work correspond to metallic Bi that exhibits a rhombohedral structure, not traces of Bi oxides or Bi alloys being observed (Fig. 2). Dissolved oxygen does not seem to incorporate either to the interface or to the Bi layer since GIXRD measurements performed with different incident angles (ω) do not present any peak assigned to oxides of Bi, Ga or As. Depending on the followed route, the Bi film has different crystallinity and morphology since film crystallinity depends on the state of the substrate surface immediately before the film growth whereas film morphology depends on the applied overpotential. Table 1 summarizes the overpotentials applied to obtain Bi layers following the three routes studied in this research.

The light route provides the most polycrystalline film as a consequence of the surface damage caused by photogenerated holes when the substrate is not completely covered by the Bi layer (Fig. 2). However, the low overpotential applied in this growth (10 mV) leads to large and well-arranged islands. The temperature route gives less polycrystalline films than the previous one because, although Bi hydroxides might be incorporated within the film, this route does not damage the substrate surface. In addition, these Bi films are quite continuous because hydrogen evolution and Bi reduction are sped up by the temperature increase. Finally, although the overpotential applied when following the scan route is higher than that applied in the light route case, the better surface condition in the former case can lead to a higher crystal quality. The film obtained in the scan route shows a Bi(012) texture which confirms that this film is the one with the highest structural quality. Hence, this route is the best among the protocols in this investigation. Nevertheless, the morphology of this film can be improved if parameters such as the growth potential or the growth mode (DC or pulsed potentiostatic electrodeposition) are optimized, which constitutes a future work.

3.5. Hydrogen readsorption

It has been verified that the light route and the scan voltage route provide compact Bi films due to the unblocking of the n-GaAs surface. However, this unblocking is temporary. If the system is left again at OCP conditions and in darkness after performing anyone of these routes, hydrogen atoms are adsorbed again at the n-GaAs surface. To confirm this point, we have performed two CVs consecutively in darkness and at 300 K (Fig. 9), leaving the system at OCP conditions just 60 s between the end of the first one (Fig. 9. a) [17] and the beginning of the second one (Fig. 9.b). The two CVs have been measured identically and as follows: they start at the OCP (100 mV for the first CV and 107 mV for the second CV), sweep

Table 1
Onset potential of Bi reduction for each studied situation. Growth potential, rms and average height of the films grown in this work.

	Blocked surface	Light route	Temperature route	Scan voltage route
Onset potential (mV)	−220	−290	−100	−130
Growth overpotential (mV)	−20	10	100	70
Rms (nm)	12	12	6	11
Average height (nm)	60	42	36	37

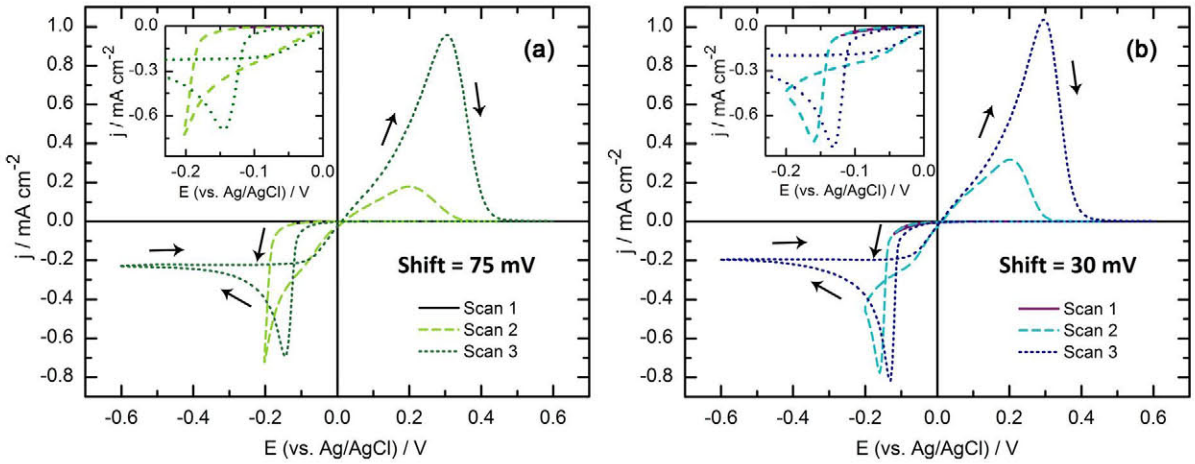

Fig. 9. a) CV scans for n-GaAs(111)B in the BiO^+ solution under dark conditions at 300 K and at a scan rate of 10 mV/s. b) CV scans performed 60 s after the end of the CV shown in Figure a.

first towards cathodic potentials till E_1 (−0.12 V for scan 1, −0.2 V for scan 2 and −0.6 V for scan 3), then towards anodic potentials till E_2 (0.3 V for scan 1, 0.45 V for scan 2 and 0.6 V for scan 3) and return to the OCP. The choice of these reverse potentials is explained in reference [17]. Although the CV in Fig. 9.a (CV1) removes the H_{ads} layer, the CV in Fig. 9.b (CV2) presents a shift between its scans, i.e. the surface is blocked again before performing CV2. The onset potential of scan 3 (assigned in our previous work to the reduction of BiO^+ ions on n-GaAs(111)B substrates) is quite similar in both CVs (E_{onset} (scan 3) ≈ −110 mV) with the exception of a little shift as a consequence of pH variation due to protons reduction [17]. However, the onset potential of scan 2 (assigned to the reduction of BiO^+ ions on the hydrogenated n-GaAs surface), is more positive in CV2 (E_{onset} (CV2, scan 2) = −135 mV) than in CV1 (E_{onset} (CV1, scan 2) = −185 mV). If the waiting time between CVs (at OCP conditions) is extended to several minutes (even one hour), the value of the shift in the second CV increases and reaches a constant value of ~40 mV, which is still lower than the shift in the first CV (~75 mV). This lower and constant value suggests that there are two sources of hydrogen adsorption. The first one is due to the charge transferred when substrate and electrolyte reach electrochemical equilibrium [17] and the second one is due to the donor character of the As-derived surface states [40]. When the substrate is immersed into the electrolyte there is adsorption due to these two effects. However, when the H_{ads} is desorbed but the system is left under OCP conditions, in darkness and at room temperature, a new adsorption takes place only due to the latter. When protons are adsorbed due to As-derived states, the H_{ads} seems to be less tightened and, therefore, it is easier to desorb it, i.e. less energy is needed. This is reflected in a more positive onset potential in the second scan (−135 mV for CV2 versus −185 mV for CV1). In addition, the dependence of the onset potential variation with the waiting time (~25 mV for 60 s and ~ 40 mV for 1 h) reflects that the amount of H_{ads} increases with time, probably until the surface is completely covered. Therefore, Bi films should be grown when hydrogen readsorption is still cancelled. When following the light route, illumination should be maintained at least during the film nucleation, despite some n-GaAs corrosion will occur. In the voltage scan route, the Bi film should be grown immediately after performing the CV scan.

4. Conclusions

In summary, we have proposed three different routes to remove the hydrogen layer adsorbed on the n-GaAs surface in order to achieve compact Bi ultra-thin films with good Bi/GaAs interfaces. In the first procedure, the electrolyte temperature has been increased to enhance Bi adatoms diffusion over the substrate surface, favoring a better atomic arrangement. However, this temperature increase leads to the formation of Bi hydroxy complexes which contribute with additional electrochemical processes. As a result, continuous but polycrystalline Bi films are obtained. The second route involves the application of light before and/or during the film growth. However, light damages the substrate surface, so this route cannot be used to obtain flat Bi ultra-thin layers with good Bi/n-GaAs interfaces at the same time. Finally, we propose to perform a CV scan just before starting the deposition of the Bi layer. This route proves the best to remove H_{ads} because it does not damage the substrate surface and does not lead to the formation of Bi hydroxy complexes. In addition, this procedure provides textured films on sufficiently low doped semiconductor substrates to perform transport measurements. We have also shown the momentary character of these routines. Hydrogen readsorption is observed if the system is left at OCP conditions, in darkness and at room temperature as a result of the interaction between As-derived surface states and the protons present into the electrolyte. Therefore, when performing the scan voltage route, it is essential to grow the Bi film immediately after performing the CV scan in order to avoid hydrogen readsorption.

Acknowledgments

We acknowledge partial financial support of this work by Spanish Ministerio de Economía y Competitividad (project MAT2011-28751-C02). Alicia Prados acknowledges financial support from Ministerio de Educación of Spain (FPU program) and acknowledges the useful discussions on this work with Dr. Ángela Llavona.

References

[1] E.I. Rogacheva, S.G. Lyubchenko, O.N. Nashchekina, A.V. Meriuts, M.S. Dresselhaus, Quantum size effects and transport phenomena in thin Bi layers, Microelectron. J. 40 (2009) 728, doi:http://dx.doi.org/10.1016/j.mejo.2008.11.007.

[2] C. Sabater, D. Gosálbez-Martínez, J. Fernández-Rossier, J.G. Rodrigo, C. Untiedt, J.J. Palacios, Topologically protected quantum transport in locally exfoliated bismuth at room temperature, Phys. Rev. B 110 (2013) , doi:http://dx.doi.org/10.1103/PhysRevLett.110.176802 176802.

[3] S. Sangiao, J.M. Michalik, L. Casado, M.C. Martínez-Velarte, L. Morellón, M.R. Ibarra, J.M. De Teresa, Conductance steps in electromigrated Bi nanoconstrictions, Phys. Chem. Chem. Phys. 15 (2013) 5132, doi:http://dx.doi.org/10.1039/c3cp44133d.

[4] M.C. Cottin, C.A. Bobisch, J. Schaffert, G. Jnawali, G. Bihlmayer, R. Möller, Interplay between forward and backward scattering of spin-orbit split surface states of Bi(111), Nano Lett. 13 (2013) 2717, doi:http://dx.doi.org/10.1021/nl400878r.

[5] M. Wada, S. Murakami, F. Freimuth, G. Bihlmayer, Localized edge states in two-dimensional topological insulators: ultrathin Bi films, Phys. Rev. B 83 (2011), doi:http://dx.doi.org/10.1103/PhysRevB.83.121310 121310(R).

[6] I.K. Drozdov, A. Alexandradinata, S. Jeon, S. Nadj-Perge, H. Ji, R.J. Cava, B.A. Bernevig, A. Yazdani, One-dimensional topological edge states of bismuth bilayers, Nat. Phys. 10 (2014) 664, doi:http://dx.doi.org/10.1038/NPHYS3048.

[7] F. Yang, L. Miao, Z.F. Wang, M.-Y. Yao, F. Zhu, Y.R. Song, M.-X. Wang, J.-P. Xu, A.V. Fedorov, Z. Sun, G.B. Zhang, C. Liu, F. Liu, D. Qian, C.L. Gao, J.-F. Jia, Spatial and energy distribution of topological edge states in single Bi(111) bilayer, Phys. Rev. Lett. 109 (2012) 016801, doi:http://dx.doi.org/10.1103/Phys.Rev.Lett.109.016801.

[8] Y.M. Koroteev, G. Bihlmayer, J.E. Gayone, E.V. Chulkov, S. Bluegel, P.M. Echenique, Ph. Hofmann, Strong spin-orbit splitting on Bi surfaces, Phys. Rev. Lett. 93 (2004) 046403, doi:http://dx.doi.org/10.1103/PhysRevLett.93.046403.

[9] T. Hirahara, K. Miyamoto, A. Kimura, Y. Niinuma, G. Bihlmayer, E.V. Chulkov, T. Nagao, I. Matsuda, S. Qiao, K. Shimada, H. Namatame, M. Taniguchi, S. Hasegawa, Origin of the surface-state band-splitting in ultrathin Bi films: from a Rashba effect to a parity effect, New J. Phys. 10 (2008) 083038, doi:http://dx.doi.org/10.1088/1367-2630/10/8/083038.

[10] A.V. Khvalkovskiy, V. Cros, D. Apalkov, V. Nikitin, M. Krounbi, K.A. Zvezdin, A. Anane, J. Grollier, A. Fert, Matching domain-wall configuration and spin-orbit torques for efficient domain-wall motion, Phys. Rev. B 87 (2013), doi:http://dx.doi.org/10.1103/PhysRevB.87.020402 020402(R).

[11] J.C. Rojas Sánchez, L. Vila, G. Desfonds, S. Gambarelli, J.P. Attanée, J.M.D. Teresa, C. Magén, A. Fert, Spin-to-charge conversion using Rashba coupling at the interface between non-magnetic materials, Nat. Commun. 4 (2013) 2944, doi:http://dx.doi.org/10.1038/ncomms3944.

[12] T.W. Cornelius, M.E. Toimil-Molares, S. Karim, R. Neumann, Oscillations of electrical conductivity in single bismuth nanowires, Phys. Rev. B 77 (2008) 125425, doi:http://dx.doi.org/10.1103/PhysRevB.77.125425.

[13] N. Marcano, S. Sangiao, M. Plaza, L. Pérez, A. Fernández Pacheco, R. Córdoba, M. C. Sánchez, L. Morellón, M.R. Ibarra, J.M. De Teresa, Weak-antilocalization signatures in the magnetotransport properties of individual electrodeposited Bi nanowires, Appl. Phys. Lett. 96 (2010) 082110, doi:http://dx.doi.org/10.1063/1.3328101.

[14] P.M. Vereecken, K. Rodbell, C. Ji, P.C. Searson, Electrodeposition of bismuth thin films on n-GaAs(110), Appl. Phys. Lett. 86 (2005) 121916, doi:http://dx.doi.org/10.1063/1.1886248.

[15] Z.L. Bao, K.L. Kavanagh, Epitaxial Bi/GaAs(111) diodes via electrodeposition, Appl. Phys. Lett. 88 (2006) 022102, doi:http://dx.doi.org/10.1063/1.2161849.

[16] P.M. Vereecken, P.C. Searson, Electrochemical formation of GaAs/Bi Schottky barriers, Appl. Phys. Lett. 75 (1999) 3135, doi:http://dx.doi.org/10.1063/1.125255.

[17] A. Prados, R. Ranchal, L. Pérez, Blocking effect in the electrodeposition of Bi on n-GaAs in acidic electrolytes, Electrochim. Acta 143 (2014) 23, doi:http://dx.doi.org/10.1016/j.electacta.2014.07.137.

[18] J.O. Bockris, S.U.M. Khan, Surface electrochemistry. A molecular level approach, Springer Science + Business Media, New York, 1993, doi:http://dx.doi.org/10.1007/978-1-4615-3040-4.

[19] A. De Vrieze, K. Strubbe, W.P. Gomes, S. Forment, R.L. Van Meirhaeghe, Electrochemical formation and properties of n-GaAs/Au and n-GaAs/Ag Schottky barriers: Influence of surface composition upon the barrier height, Phys. Chem. Chem. Phys. 3 (2001) 5297, doi:http://dx.doi.org/10.1039/b104887m.

[20] G. Oskam, D. Vanmaekelbergh, J.J. Kelly, The influence of electrodeposited gold on the properties of III-V semiconductor electrodes -part 1. Results of current-potential measurements on p-GaAs, Electrochim. Acta 38 (1993) 291, doi:http://dx.doi.org/10.1016/0013-4686(93)85142-L.

[21] A. Holleman, E. Wiberg, N. Wiberg, Holleman-Wieberg: Inorganic Chemistry, Academic Press, London, 2001.

[22] Z. Borkowska, U. Slimming, Perchlorate adsorption on polycrystalline gold electrodes in aqueous perchloric acid, J. Electroanal. Chem. 312 (1991) 237, doi:http://dx.doi.org/10.1016/0022-0728(91)85156-J.

[23] O. Koga, Y. Watanabe, M. Tanizaki, Y. Hori, Specific adsorption of anions on a copper (100) single crystal electrode studied by charge desplacement by CO adsorption and infrared spectroscopy, Electrochim. Acta 46 (2001) 3083, doi:http://dx.doi.org/10.1016/S0013-4686(01)00599-0.

[24] P.M. Vereecken, L. Sun, P.C. Searson, M. Tanase, D.H. Reich, C.L. Chien, Magnetotransport properties of bismuth films on p-GaAs, J. Appl. Phys. 88 (2000) 6529, doi:http://dx.doi.org/10.1063/1.1323537.

[25] B. Lovrecek, I. Mekjavic, M. Metikos-Hukovic, Bismuth, in: A.J. Bard, R. Parsons, J. Jordan (Eds.), Standard Potentials in Aqueous Solutions, International Union of Pure and Applied Chemistry, New York, 1985 p. 180.

[26] A. Olin, Studies on the Hydrolysis of Metal Ions. 19. The hydrolysis of bismuth (III) in perchlorate medium, Acta Chem. Scand. 11 (1957) 1445, doi:http://dx.doi.org/10.3891/acta.chem.scand.11-1445.

[27] B.H. Erné, F. Ozanam, J.-N. Chazalviel, The mechanism of hydrogen gas evolution on GaAs cathodes elucidated by in situ infrared spectroscopy, J. Phys. Chem. B 103 (1999) 2948, doi:http://dx.doi.org/10.1021/jp984765t.

[28] W.J. Pielth, G. Pfuhl, A. Felske, W. Badawy, Photoetching of III/V semiconductors, Electrochim. Acta 34 (1989) 1133, doi:http://dx.doi.org/10.1016/0013-4686(89)87146-4.

[29] W.P. Gomes, H.H. Goossens, Electrochemistry of III-V compound semiconductors: dissolution kinetics and etching, in: H. Gerischer, C.W. Tobias (Eds.), Advances in Electrochemical Science and Engineering, vol. 3, VCH Verlagsgesellschaft mbH, Weinheim, 1994, doi:http://dx.doi.org/10.1002/maco.19950460317 p. 5.

[30] H. Gerischer, Electrochemical behaviour of semiconductors under illumination, J. Electrochem. Soc. 113 (1966) 1174, doi:http://dx.doi.org/10.1149/1.2423779.

[31] J. Li, L.M. Peter, Surface recombination at semiconductor electrodes. Part IV. Steady-state and intensity modulated photocurrents at n-GaAs electrodes, J. Electro Anal. Chem. (1986) 199, doi:http://dx.doi.org/10.1016/0022-0728(86)87038-3.

[32] Y. Huang, J. Luo, D.G. Ivey, Comparative study of GaAs corrosion in H_2SO_4 and NH_3H_2O solutions by electrochemical methods and surface analysis, Mat. Chem. Phys. 93 (2005) 429, doi:http://dx.doi.org/10.1016/j.matchemphys.2005.03.049.

[33] R. Memming, Semiconductor Electrochemistry, Wiley-VCH Verlag GmbH, Weinheim, 2001, doi:http://dx.doi.org/10.1002/9783527613069.

[34] B.H. Erné, F. Ozanam, J.-N. Chazalviel, Dynamics of Hydrogen Adsorption on GaAs Electrodes, Phys. Rev. Lett. 80 (1998) 4337, doi:http://dx.doi.org/10.1103/PhysRevLett.80.

[35] B.H. Erné, M. Stchakovsky, F. Ozanam, J.-N. Chazalviel, Surface Composition of n-GaAs Cathodes during Hydrogen Evolution Characterized by In Situ Ultraviolet-Visible Ellipsometry and In Situ Infrared Spectroscopy, J. Electrochem. Soc. 145 (1998) 447, doi:http://dx.doi.org/10.1149/1.1838283.

[36] J.M. Woodall, P. Oelhafen, T.N. Jackson, J.L. Freeouf, G.D. Pettit, Photoelectrochemical passivation of GaAs surfaces, J. Vac. Sci. Technol. B 1 (1983) 795, doi:http://dx.doi.org/10.1116/1.582680.

[37] M.S. Antelman, F.J. Harris Jr., The Encyclopedia of Chemical Electrode Potentials, Plenum Press, New York, 1982, pp. 98, doi:http://dx.doi.org/10.1007/978-1-4613-3374-6.

[38] T. Mitsunaga, X-ray thin-film measurement techniques. II Out-of-plane diffraction measurements, The Rigaku J. 25 (2009) 7.

[39] H. Gerischer, W. Mindt, The mechanism of the decomposition of semiconductors by electrochemical oxidation and reduction, Electrochim. Acta 13 (1968) 1329, doi:http://dx.doi.org/10.1016/0013-4686(68)80060-X.

[40] H. Lüth, Surface and Interfaces of Solid Materials, Springer-Verlag, Berlin, 1995, doi:http://dx.doi.org/10.1002/crat.2170310203.